JCI The Journal of Clinical Investigation

Long-range *cis*-regulatory elements controlling *GDF6* expression are essential for cochlear development

Guney Bademci, … , Katherina Walz, Mustafa Tekin

J Clin Invest. 2020. https://doi.org/10.1172/JCI136951.

Concise Communication In-Press Preview Genetics Otology

Graphical abstract

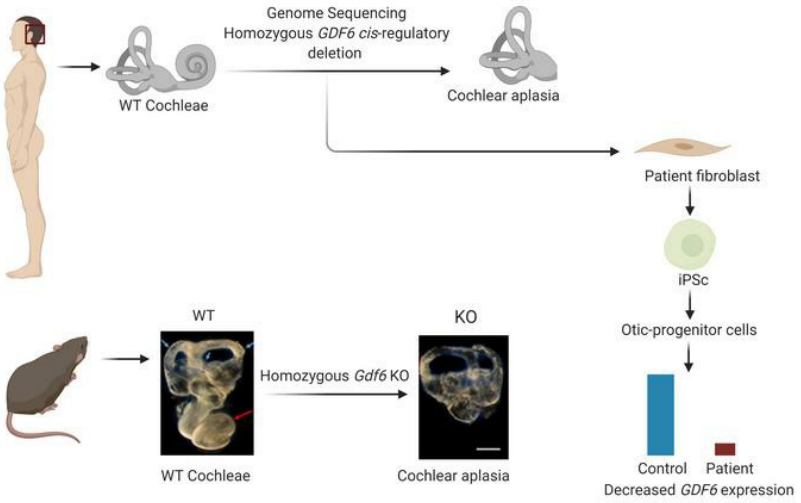

Long-range *cis*-regulatory elements controlling *GDF6* expression are essential for cochlear development

Guney Bademci[1], Clemer Abad[1], Filiz B. Cengiz[1], Serhat Seyhan[1], Armagan Incesulu[2], Shengru Guo[1], Suat Fitoz[3], Emine Ikbal Atli[4], Nicholas C. Gosstola[1], Selma Demir[4], Brett M. Colbert[1,5], Gozde Cosar Seyhan[6], Claire J. Sineni[1], Duygu Duman[7], Hakan Gurkan[4], Cynthia C. Morton[8,9,10,11,12], Derek M Dykxhoorn[1,13], Katherina Walz[1,13], Mustafa Tekin[1,13,14*]

1) John P. Hussman Institute for Human Genomics, University of Miami Miller School of Medicine, Miami, FL 33136, USA.

2) Department of Otolaryngology, Eskisehir Osmangazi University School of Medicine, Eskisehir, Turkey.

3) Department of Diagnostic Radiology, Ankara University School of Medicine, Ankara, Turkey.

4) Department of Medical Genetics, Trakya University, Faculty of Medicine, Edirne, Turkey.

5) Medical Scientist Training Program, Miller School of Medicine, Miami, Florida 33136, USA.

6) Department of Dermatology, Bakirkoy Sadi Konuk Training and Research Hospital, Istanbul, Turkey.

7) Department of Audiology, Ankara University School of Medicine, Ankara, 06100, Turkey.

8) Department of Obstetrics and Gynecology, Brigham and Women's Hospital, Boston, MA 02115, USA.

9) Harvard Medical School, Boston, MA 02115, USA.

10) Program in Medical and Population Genetics, Broad Institute of MIT and Harvard, Cambridge, MA 02142, USA.

11) Department of Pathology, Brigham and Women's Hospital, Boston, MA 02115, USA.

12) Manchester Centre for Audiology and Deafness, School of Health Sciences, Faculty of Biology, Medicine and Health, University of Manchester, Manchester Academic Health Science Centre, Manchester M13 9NT, UK.

13) Dr. John T. Macdonald Foundation Department of Human Genetics, University of Miami Miller School of Medicine, Miami, FL 33136, USA.

14) Department of Otolaryngology, University of Miami Miller School of Medicine, Miami, FL 33136, USA.

***Corresponding Author:**
Mustafa Tekin, M.D.
1501 NW 10th Avenue, BRB-610 (M-860), Miami, FL, 33136
Phone: 305-243-2381
Fax: 305-243-2704
Email: mtekin@med.miami.edu

Conflict of interest: The authors have declared that no conflict of interest exists.

Abstract

Molecular mechanisms governing the development of mammalian cochlea, the hearing organ, remain largely unknown. Through genome sequencing in three subjects from two families with non-syndromic cochlear aplasia, we identified homozygous 221 KB and 338 KB deletions in a non-coding region on chromosome 8 with an ~200 KB overlapping section. Genomic location of the overlapping deleted region was starting from ~350 KB downstream of *GDF6*. Otic lineage cells differentiated from induced pluripotent stem cells derived from an affected individual show reduced expression of *GDF6* compared to control cells. A mouse knock-out of *Gdf6* reveals cochlear aplasia closely resembling the human phenotype. We conclude that GDF6 plays a necessary role in early cochlear development controlled by cis-regulatory elements located within ~500 KB region of the genome in humans and that its disruption leads to deafness due to cochlear aplasia.

Key words

Cochlear aplasia, GDF6, hearing loss, inner ear anomaly, non-coding variant

Introduction

The inner ear is a complex organ that arises through a series of morphogenetic events from a simple embryologic structure, the otocyst. It consists of a dorsal vestibular system and a ventral auditory component that forms the cochlea. The cochlea houses hair cell auditory receptors, which translate sound into electrical signals deciphered by the brain (1, 2). Inner ear development requires a highly orchestrated process to establish otic identity in early development, including modeling the structure with morphogenetic movements, expression of cell specific proteins, and differentiation of the highly specialized cell types (1, 3). While model animals have been used to elucidate pathways and genes involved in these processes, the molecular mechanisms that govern early cochlear development in humans are poorly understood.

Hearing loss (HL) is the most common sensory deficit affecting almost half of all people at some time in their lives. Clinically significant hearing loss is present in ~1 per 500 newborns (4). Inner ear malformations, detected by a computerized tomography or magnetic resonance imaging, are diagnosed in up to 25% of children with HL (5). One-third of these children have severe cochlear malformations associated with profound sensorineural HL (6). Cochlear malformations can be a phenotypic finding in a recognizable multisystemic condition, such as Pendred (MIM 274600), branchiootorenal (MIM 113650), or CHARGE (MIM 214800) syndromes. Majority of cochlear malformations, however, are isolated without additional findings. DNA variants in very few genes have been reported to cause non-syndromic HL associated with cochlear malformations (2, 7-10).

During embryonic development, tightly regulated gene expression in time and space is essential to shape a highly complex organism from a single cell. To achieve the required precision, core promotors close to transcription start sites must interact with non-coding regulatory elements in their vicinity, termed enhancers (11). Enhancers and promotors communicate across large genomic distances by getting physical contacts via chromatin folding. A small number of non-coding DNA variants disrupting enhancers have been discovered in patients with congenital malformations (11). In this study, we aimed to determine molecular components of early cochlear development by undertaking a genetic study on congenital deafness associated with cochlear aplasia.

Results and Discussion

We studied three affected and eight unaffected individuals from two Turkish families (**Figure 1, A and B**). The proband (Individual IV:4 in **Figure 1A**) in Family 1 is a 20 year-old male who was born with profound deafness to healthy consanguineous parents. His cousin, another 20 year-old male (IV:1 in **Figure 1A**), was

born deaf as well. The proband in Family 2 is an 18 year-old male (IV:1 in **Figure 1B**) who is also profoundly deaf. Pure tone audiograms in all three individuals show profound sensorineural HL. Thorough clinical evaluations, including ophthalmological studies, have shown no additional findings, suggesting non-syndromic deafness. Specifically, these affected individuals did not have any skeletal abnormalities in their extremities nor in their spine upon clinical examination, which was confirmed by X-rays. Development of gross motor skills was normal and a clinical examination showed normal tandem walking with a negative Romberg's test, suggesting an intact vestibular system. Computerized tomography and magnetic resonance imaging of the temporal bone revealed cochlear aplasia in all three individuals with normal appearing vestibular systems **(Figure 1C)**.

DNA samples from two affected individuals along with their normal hearing siblings and parents in Family 1 and from the proband in Family 2 underwent genome sequencing. On average, read depth was 37.34X; 1X and 10X coverage were 99.37% and 99.04%, respectively **(Supplemental Table 1)**.

We first evaluated the genomes of the three affected individuals separately for all known deafness genes [retrieved from Hereditary Hearing Loss Homepage (http://hereditaryhearingloss.org/) and Online Mendelian Inheritance in Man (OMIM)(https://www.omim.org)] following recently published guidelines (12). This analysis did not reveal a plausible variant in any subject under any inheritance model. We subsequently evaluated single nucleotide variants (SNVs) and indels in the entire Family 1 mapping to runs of homozygosity (>2 MB) shared by both affected individuals **(Supplemental Table 2, 3, and 4)** and had an allele frequency of < 0.0007 in gnomAD (global allele frequency) (12). From this list, we selected variants for which all four parents were heterozygous and the unaffected siblings were not homozygous for the variant allele. This analysis yielded 32 variants **(Supplemental Table 5).** None of these variants mapped to protein coding regions; they were not located at conserved DNA sites (phastCons conservation >0.4 for vertebrates and mammals; http://compgen.cshl.edu/phast/phastCons-tutorial.php#dnc); nor were they predicted to have an effect on gene function **(Supplemental Table 5)**. We then checked segregating copy number variants (CNVs), which yielded only a single deletion, Chr8:96,582,049-96,803,788 (221,739 bp; hg19), in Family 1 **(Supplemental Table 6)**. This region was in the longest homozygous run (5.4 MB) shared by the two affected individuals in Family 1. The same locus was within an 18.2 MB homozygous run in the proband of Family 2, who was homozygous for an overlapping deletion: Chr8:96,596,661-96,934,796 (338,135 bp; hg19). Sanger sequencing illuminated breakpoints of both deletions **(Supplemental Figure 1)**. We confirmed the presence and segregation of both deletions, seq[GRCh37] del(8)(q22.1(96,582,048)::q22.1(96,803,789)) for Family 1 and seq[GRCh37] del(8)(q22.1(96,596,660)::G::q22.1(96,934,797)) for Family 2 using primer pairs specific for deletions via PCR **(Figure 1, A and B, Supplemental Table 7)**. These large deletions are not present on gnomAD

(https://gnomad.broadinstitute.org/), Database of Genomic Variants (http://dgv.tcag.ca/dgv/app/home), or DECIPHER (https://decipher.sanger.ac.uk/browser). Screening of each deletion in an additional 1,025 unrelated Turkish individuals was negative, suggesting that these deletions are not common in the Turkish population. The single locus two-point LOD score calculated using Superlink (13) with a disease allele frequency of 0.001 under a fully penetrant autosomal recessive model in the two families is 4.46.

Topologically associating domain (TAD) analysis of the deleted region shows that both deletions are in the same TAD as *GDF6* (MIM 601147) **(Figure 2A)**. To demonstrate that *GDF6* is involved in cochlear development, we undertook experiments to differentiate otic lineage cells from human iPSCs. To determine if there were expression differences between affected and control individuals, we derived iPSCs from the fibroblasts of the proband in Family 1 and two age and sex-matched controls. These affected and unaffected control iPSCs were differentiated into early otic lineage cells, nonneuronal ectoderm (NNE) and preplacodal ectoderm (PPE) cells, following an established stepwise differentiation protocol **(Figure 2B)** (14). We determined the expression of specific markers in different stages with immunocytochemistry, RNA sequencing, and quantitative reverse transcriptase (RT)-PCR **(Figure 2B and Supplemental Figure 2)**.

RNA-seq and (RT)-PCR revealed that *GDF6* expression was absent on day 3 (iPSC) both in the patient-specific and control cells. There was an increase in *GDF6* expression on day 6 (NNE) and 11 (PPE) post-initiation of differentiation in both the patient-specific and control cells **(Figure 2B)**; the *GDF6* mRNA levels were significantly lower in the patient-specific cells compared to those of the controls on day 11 **(Figure 2B and Supplemental Figure 3)**. Moreover, none of the 13 genes within 1 MB of the overlapping deletion region showed any significant differences in expression **(Supplemental Figure 4)**. These results suggest that *GDF6* expression begins during the early stages of inner ear development and that the deletion on chromosome 8 reduces its expression. Analysis of the deleted region shows multiple highly conserved DNA sequences and active chromatin positions, suggesting that this region contains enhancers for the regulation of gene expression **(Figure 2A and Supplemental Figure 5)** (15, 16).

Finally, to show that disruption of Gdf6 affects cochlear development, we evaluated a *Gdf6* knock-out mouse model. *Gdf6* knock-out (*Gdf6*$^{-/-}$) mice do not survive postnatally and show fusion of the carpal and tarsal joints, coronal craniosynostosis, and middle ear defects (17). An inner ear phenotype in *Gdf6* knock-out mice has not been reported. First, we showed that *Gdf6* is highly expressed in the cochlea during development and in adult mice **(Supplemental Figure 6)**. We subsequently dissected *Gdf6* mutant mouse inner ears followed by paint-filling to assess anomalies indicative of the human phenotype. **Figure 2, C-E** show defects in the mutant mice with cochlear aplasia, while the vestibular anatomy is normal.

The 207,127 bp deletion region on human chromosome 8 corresponds to 219,606 bp of mouse chromosome 4 between 10,250,649-10,470,254 bps (GRCm38). 11% of these sequences are conserved in mammalians and are identical between humans and mice **(Supplemental Figure 7).**

In this study we show that homozygous deletions removing putative enhancers of *GDF6* lead to non-syndromic HL associated with cochlear aplasia. *GDF6* codes for growth and differentiation factor 6, a member of the transforming growth factor-beta superfamily within the bone morphogenic protein (BMP) family. It has been shown to play a role in normal formation of bones and joints in the limbs, skull, and axial skeleton (18). Heterozygous SNVs in *GDF6* have been reported in multiple synostosis syndrome (MIM 617898)(19), microphthalmia (MIM 613094)(20), and Klippel-Feil syndrome (MIM 118100) characterized by fused cervical vertebrae and a short neck, sometimes associated with sensorineural deafness.(21) Three missense gain of function variants were shown to cause multiple synostosis syndrome by increasing the potency of GDF6 as a BMP signal (19, 22, 23). A clear loss of function effect of the other reported amino acid substitutions has not been demonstrated and their roles in monogenic congenital anomalies have been debated (22).

It has been proposed that expression of *GDF6* is controlled by many tissue-specific enhancers that function during embryogenesis (24). Enhancers within ~100 KB region flanking *Gdf6* have been shown to control limb development (18). Deletions detected in our study map to a ~ 900 KB region in the 3′ of *GDF6* , which is a gene desert, a genomic region that is frequently associated with regulatory elements controlling expression of neighboring genes during embryonic development (24, 25). Multiple enhancers acting on the same promotor controlling differing spatiotemporal expression of the gene have been well described (11). Typically, enhancer-promotor interactions are complex due to the existence of multiple redundant enhancers with overlapping activities. A phenotypic manifestation in these cases can only be observed when variants disturb multiple enhancers (26). In rare instances, loss of a single enhancer may lead to a phenotype. For example, at least 11 enhancers driving the expression of *Shh* in different tissues, such as central nervous system, epithelial lining, and limbs were reported (27). Removal of the limb-specific *ZRS* enhancer eliminates *Shh* expression only in the limbs affecting limb outgrow (27).

It has been recently shown that a ~123 KB deletion within the mouse *Slc25a13* gene on chromosome 5 is associated with reduced transcription of *Dlx5,* which is located in cis 660 KB away. *Dlx5 is* known to play role in inner ear development and remarkably the *Slc25a13* mutant mice showed inner ear anomalies similar to $Dlx5^{-/-}$ animals, reinforcing the concept of being a long-range *Dlx5* enhancer (28). Similarly,

deletions within a 1 MB region upstream of *POU3F4* on the X chromosome have been detected in patients with cochlear anomalies, suggesting the presence of cis-acting regulatory elements in the deleted regions (29).

The overlapping deletion region also includes the 3` end of a long ncRNA (C8orf37-AS1). We did not detect RNA of this long ncRNA in control iPSCs or in otic lineage cells. We also did not observe a difference in the expression of *C8orf37* (**Supplemental Figure 4**). Further studies are needed to confirm the existence and characterization of this long ncRNA.

It is of interest that we observed only cochlear aplasia with an intact vestibule in the *Gdf6*$^{-/-}$ mice. While *Gdf6* is expressed both in the cochlea and vestibule of developing and adult mice **(Supplemental Figure 8)** (30), its expression is more pronounced in the cochlea. It is possible that the lack of vestibular *Gdf6* in the *Gdf6*$^{-/-}$ is compensated by other genes. We propose that the overlapping deletions we detected in three patients leave *GDF6* as well as other regulatory elements located outside of the deleted regions intact, and thus lead only to non-syndromic deafness. It will be interesting to determine if cochlear aplasia is due to the deletion of only one enhancer or the combined effects of multiple enhancers mapping to the deleted region.

Methods

Complete details on the experimental materials and methods are provided in the supplemental materials.

Genome and RNA sequencing data are available at NCBI BioProject: PRJNA623118 (BioSample: SAMN14539183 and SAMN14539184) and BioProject: PRJNA626451 respectively.

Study approval

This study was approved by the Ethics Committee of Ankara University in Turkey (012413) and the Institutional Review Board at the University of Miami in the USA (20081138). A signed informed consent form was obtained from each participant or, in the case of a minor, from parents.

All procedures were approved by the University of Miami Institutional Animal Care and followed the NIH Guidelines, "Using Animals in Intramural Research".

Statistics. Differences between mRNA levels of patient and control samples were compared with nonparametric test (Mann-Whitney U test with independent variables). A p value of less than 0.05 was considered significant.

Author contributions

Study design: M.T. Clinical evaluation and sample collection: A.I., S.D., D.D., H.G., S.S., G.C.S., E.I.A., S.F., and M.T. Methods and data analysis: G.B., C.A., F.B.C., S.S., S.G., N.C.G, B.M.C., and C.J.S. Mouse knockout model: C.A. and K.W. Experimental and analytical supervision: D.M.D., K.W., and M.T. Writing: G.B., C.A., D.M.D., K.W., C.C.M., and M.T., and all co-authors reviewed the manuscript.

Acknowledgements

This work was supported by National Institutes of Health R01DC009645 and R01DC012836 to M.T. and R01DC015052 to C.C.M., and the University of Manchester National Institute for Health Research Biomedical Research Centre to C.C.M.

References

1. Wu DK, and Kelley MW. Molecular mechanisms of inner ear development. *Cold Spring Harb Perspect Biol.* 2012;4(8):a008409.
2. Diaz-Horta O, Abad C, Sennaroglu L, Foster J, 2nd, DeSmidt A, Bademci G, et al. ROR1 is essential for proper innervation of auditory hair cells and hearing in humans and mice. *Proc Natl Acad Sci U S A.* 2016;113(21):5993-8.
3. Whitfield TT. Development of the inner ear. *Curr Opin Genet Dev.* 2015;32:112-8.
4. Morton CC, and Nance WE. Newborn hearing screening--a silent revolution. *N Engl J Med.* 2006;354(20):2151-64.
5. Mafong DD, Shin EJ, and Lalwani AK. Use of laboratory evaluation and radiologic imaging in the diagnostic evaluation of children with sensorineural hearing loss. *Laryngoscope.* 2002;112(1):1-7.
6. McClay JE, Booth TN, Parry DA, Johnson R, and Roland P. Evaluation of pediatric sensorineural hearing loss with magnetic resonance imaging. *Arch Otolaryngol Head Neck Surg.* 2008;134(9):945-52.
7. Tekin M, Hismi BO, Fitoz S, Ozdag H, Cengiz FB, Sirmaci A, et al. Homozygous mutations in fibroblast growth factor 3 are associated with a new form of syndromic deafness characterized by inner ear agenesis, microtia, and microdontia. *Am J Hum Genet.* 2007;80(2):338-44.
8. Everett LA, Glaser B, Beck JC, Idol JR, Buchs A, Heyman M, et al. Pendred syndrome is caused by mutations in a putative sulphate transporter gene (PDS). *Nat Genet.* 1997;17(4):411-22.
9. Bademci G, Abad C, Incesulu A, Elian F, Reyahi A, Diaz-Horta O, et al. FOXF2 is required for cochlear development in humans and mice. *Hum Mol Genet.* 2019;28(8):1286-97.
10. Schrauwen I, Kari E, Mattox J, Llaci L, Smeeton J, Naymik M, et al. De novo variants in GREB1L are associated with non-syndromic inner ear malformations and deafness. *Hum Genet.* 2018;137(6-7):459-70.
11. Robson MI, Ringel AR, and Mundlos S. Regulatory Landscaping: How Enhancer-Promoter Communication Is Sculpted in 3D. *Mol Cell.* 2019;74(6):1110-22.
12. Oza AM, DiStefano MT, Hemphill SE, Cushman BJ, Grant AR, Siegert RK, et al. Expert specification of the ACMG/AMP variant interpretation guidelines for genetic hearing loss. *Hum Mutat.* 2018;39(11):1593-613.

13. Silberstein M, Weissbrod O, Otten L, Tzemach A, Anisenia A, Shtark O, et al. A system for exact and approximate genetic linkage analysis of SNP data in large pedigrees. *Bioinformatics.* 2013;29(2):197-205.
14. Matsuoka AJ, Morrissey ZD, Zhang C, Homma K, Belmadani A, Miller CA, et al. Directed Differentiation of Human Embryonic Stem Cells Toward Placode-Derived Spiral Ganglion-Like Sensory Neurons. *Stem Cells Transl Med.* 2017;6(3):923-36.
15. Gao T, He B, Liu S, Zhu H, Tan K, and Qian J. EnhancerAtlas: a resource for enhancer annotation and analysis in 105 human cell/tissue types. *Bioinformatics.* 2016;32(23):3543-51.
16. Wang Y, Song F, Zhang B, Zhang L, Xu J, Kuang D, et al. The 3D Genome Browser: a web-based browser for visualizing 3D genome organization and long-range chromatin interactions. *Genome Biol.* 2018;19(1):151.
17. Settle SH, Rountree RB, Sinha A, Thacker A, Higgins K, and Kingsley DM. Multiple joint and skeletal patterning defects caused by single and double mutations in the mouse Gdf6 and Gdf5 genes. *Developmental Biology.* 2003;254(1):116-30.
18. Indjeian VB, Kingman GA, Jones FC, Guenther CA, Grimwood J, Schmutz J, et al. Evolving New Skeletal Traits by cis-Regulatory Changes in Bone Morphogenetic Proteins. *Cell.* 2016;164(1-2):45-56.
19. Wang J, Yu T, Wang Z, Ohte S, Yao RE, Zheng Z, et al. A New Subtype of Multiple Synostoses Syndrome Is Caused by a Mutation in GDF6 That Decreases Its Sensitivity to Noggin and Enhances Its Potency as a BMP Signal. *J Bone Miner Res.* 2016;31(4):882-9.
20. Asai-Coakwell M, French CR, Berry KM, Ye M, Koss R, Somerville M, et al. GDF6, a novel locus for a spectrum of ocular developmental anomalies. *Am J Hum Genet.* 2007;80(2):306-15.
21. Tassabehji M, Fang ZM, Hilton EN, McGaughran J, Zhao Z, de Bock CE, et al. Mutations in GDF6 are associated with vertebral segmentation defects in Klippel-Feil syndrome. *Hum Mutat.* 2008;29(8):1017-27.
22. Terhal PA, Verbeek NE, Knoers N, Nievelstein R, van den Ouweland A, Sakkers RJ, et al. Further delineation of the GDF6 related multiple synostoses syndrome. *Am J Med Genet A.* 2018;176(1):225-9.
23. Drage Berentsen R, Haukanes BI, Juliusson PB, Rosendahl K, and Houge G. A Novel GDF6 Mutation in a Family with Multiple Synostoses Syndrome without Hearing Loss. *Mol Syndromol.* 2019;9(5):228-34.
24. Pregizer S, and Mortlock DP. Control of BMP gene expression by long-range regulatory elements. *Cytokine Growth Factor Rev.* 2009;20(5-6):509-15.
25. Ovcharenko I, Loots GG, Nobrega MA, Hardison RC, Miller W, and Stubbs L. Evolution and functional classification of vertebrate gene deserts. *Genome Res.* 2005;15(1):137-45.
26. Osterwalder M, Barozzi I, Tissieres V, Fukuda-Yuzawa Y, Mannion BJ, Afzal SY, et al. Enhancer redundancy provides phenotypic robustness in mammalian development. *Nature.* 2018;554(7691):239-43.
27. Anderson E, Devenney PS, Hill RE, and Lettice LA. Mapping the Shh long-range regulatory domain. *Development.* 2014;141(20):3934-43.
28. Johnson KR, Gagnon LH, Tian C, Longo-Guess CM, Low BE, Wiles MV, et al. Deletion of a Long-Range Dlx5 Enhancer Disrupts Inner Ear Development in Mice. *Genetics.* 2018;208(3):1165-79.
29. Naranjo S, Voesenek K, de la Calle-Mustienes E, Robert-Moreno A, Kokotas H, Grigoriadou M, et al. Multiple enhancers located in a 1-Mb region upstream of POU3F4 promote expression during inner ear development and may be required for hearing. *Hum Genet.* 2010;128(4):411-9.
30. Rudnicki A, Isakov O, Ushakov K, Shivatzki S, Weiss I, Friedman LM, et al. Next-generation sequencing of small RNAs from inner ear sensory epithelium identifies microRNAs and defines regulatory pathways. *BMC Genomics.* 2014;15:484.

Figure Legends

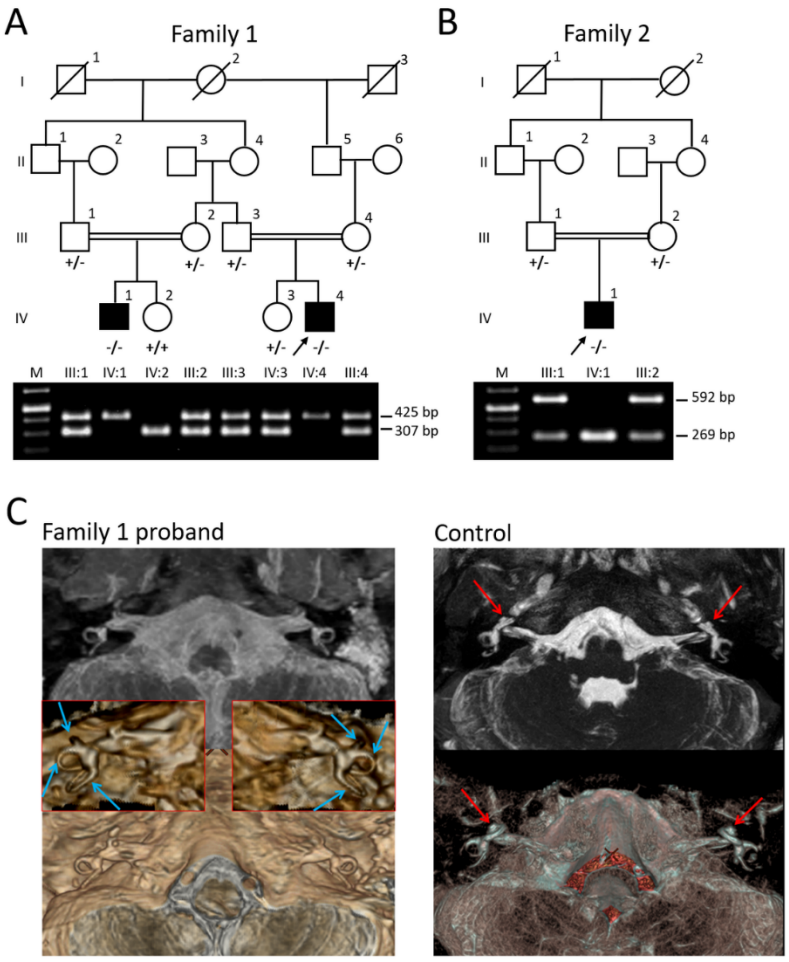

Figure 1: Clinical features and variant information. (A and B) Pedigrees of the studied families with segregation of detected deletions. -/-: homozygous deletion, +/-: heterozygous deletion, +/+: homozygous wildtype; M: 1 KB ladder, amplicons of deletion specific primers are 425 bp and 269 bp in families 1 and 2, respectively; amplicons of wildtype specific primers are 307 bp and 592 bp in families 1 and 2, respectively. **(C)** Heavily T2-weighted MRI of temporal bone, axial maximum intensity projection and volume rendered images when the proband of Family 1 was 9 years old showing complete absence of the cochlea. Vestibule and semicircular canals (blue arrows) are of normal shape and caliper. Control: MRI of a normal 9 year-old male reveals normal cochleae (red arrows) and semicircular canals.

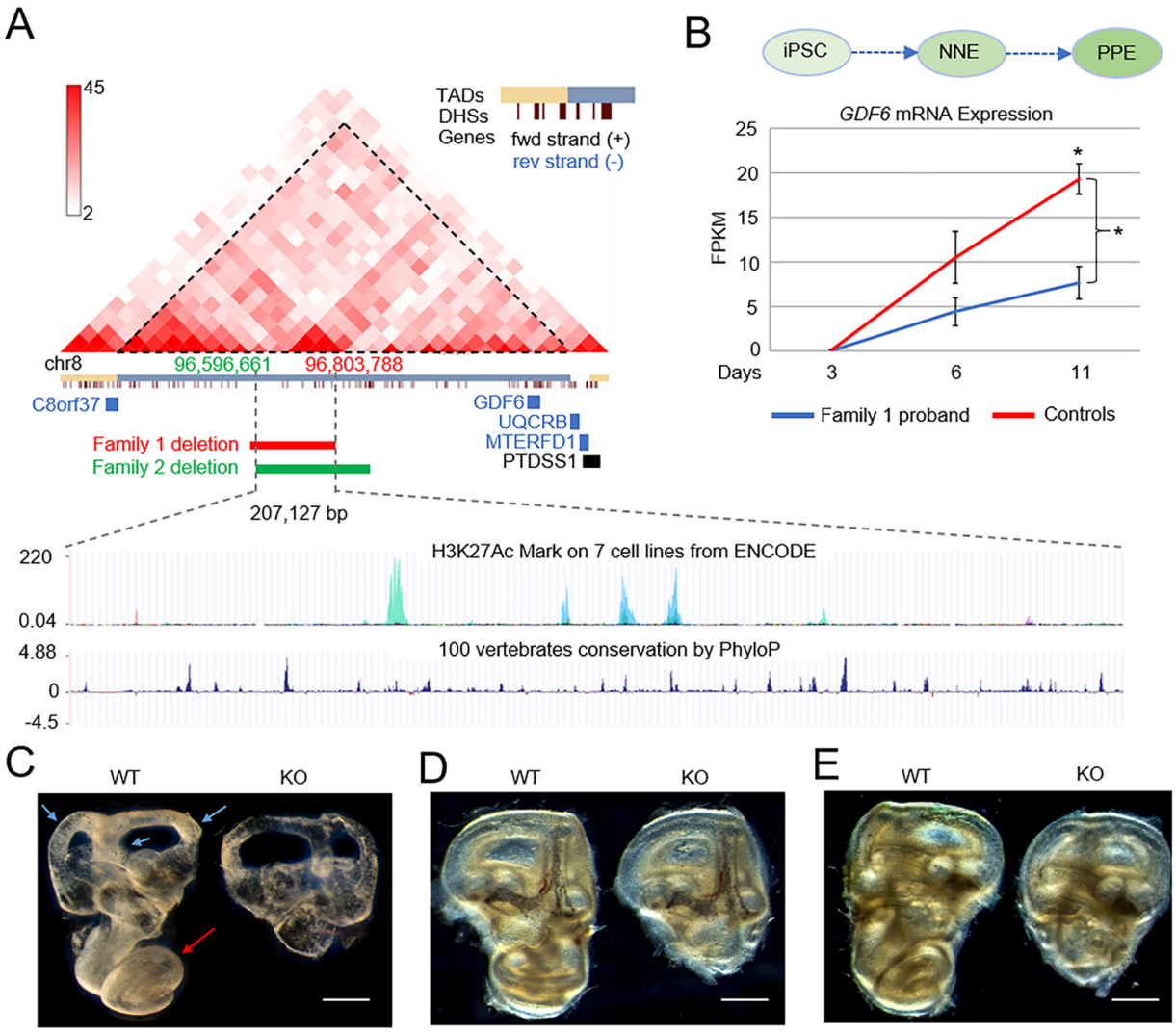

Figure 2: Deleted genomic region, mRNA expression, and mouse studies. **(A)** A topologically associating domain (TAD) on chromosome 8 including detected deletions (3D Genome Browser; http://promoter.bx.psu.edu/hi-c/chic.php). Boundaries of the TAD are shown with a blue bar under a triangle marked with dotted lines. The overlapping deletion is 207,127 bp shown with vertical dotted lines. This region contains multiple higher activation of transcription sites demonstrated by active enhancer mark H3K27Ac and DNAse I hypersensitive sites (DHS); the deleted region also includes multiple highly conserved DNA sequences as shown by PhyloP scores. **(B)** *GDF6* mRNA levels during differentiation from iPSCs. NNE: non-neural ectoderm cells; PPE: preplacodal ectoderm cells. Data are represented as means ± SEM (n=4 cases; n=4 controls). *For day 11 mRNA levels and areas under the curve between patient-derived and control cells are significantly different (p=0.029). Mann-Whitney U test with independent variables was used for comparisons. FPKM: Fragments Per Kilobase of transcript per Million mapped reads. **(C, D and E)** Cochlear aplasia in *Gdf6* mutant mice. **(C)** Paint fill of P0 mouse inner ear for WT and KO mice. The red arrow indicates normal cochlear morphology and blue arrows show semicircular canals. **(D and E)** Bright field photographs of the whole dissected inner ear at P0 from different angles. Note that the *Gdf6* mutant lacks the entire cochlea. Scale bar: 500 µm. WT: Wildtype, KO: Knock-out